THE JOURNAL OF BIOLOGICAL CHEMISTRY
Vol. 279, No. 25, Issue of June 18, pp. 26370–26377, 2004

Printed in U.S.A.

A Kazal-like Extracellular Serine Protease Inhibitor from *Phytophthora infestans* Targets the Tomato Pathogenesis-related Protease P69B*

Received for publication, January 28, 2004, and in revised form, April 15, 2004
Published, JBC Papers in Press, April 19, 2004, DOI 10.1074/jbc.M400941200

Miaoying Tian, Edgar Huitema, Luis da Cunha, Trudy Torto-Alalibo, and Sophien Kamoun‡

From the Department of Plant Pathology, The Ohio State University, Ohio Agricultural Research and Development Center, Wooster, Ohio 44691

The oomycetes form one of several lineages within the eukaryotes that independently evolved a parasitic lifestyle and consequently are thought to have developed alternative mechanisms of pathogenicity. The oomycete *Phytophthora infestans* causes late blight, a ravaging disease of potato and tomato. Little is known about processes associated with *P. infestans* pathogenesis, particularly the suppression of host defense responses. We describe and functionally characterize an extracellular protease inhibitor, EPI1, from *P. infestans*. EPI1 contains two domains with significant similarity to the Kazal family of serine protease inhibitors. Database searches suggested that Kazal-like proteins are mainly restricted to animals and apicomplexan parasites but appear to be widespread and diverse in the oomycetes. Recombinant EPI1 specifically inhibited subtilisin A among major serine proteases and inhibited and interacted with the pathogenesis-related P69B subtilisin-like serine protease of tomato in intercellular fluids. The *epi1* and *P69B* genes were coordinately expressed and up-regulated during infection of tomato by *P. infestans*. Inhibition of tomato proteases by EPI1 could form a novel type of defense-counterdefense mechanism between plants and microbial pathogens. In addition, this study points to a common virulence strategy between the oomycete plant pathogen *P. infestans* and several mammalian parasites, such as the apicomplexan *Toxoplasma gondii*.

Parasitic and pathogenic lifestyles have evolved repeatedly in eukaryotes (1). Several parasitic eukaryotes represent deep phylogenetic lineages, suggesting that they feature unique molecular processes for infecting their hosts. One such lineage is formed by the oomycetes, a group of fungus-like organisms that are distantly related to fungi but closely related to brown algae and diatoms in the Stramenopiles (1–3). One of the most notorious and destructive oomycete is the Irish famine pathogen, *Phytophthora infestans*. This species causes late blight, a reemerging and ravaging disease of potato and tomato (4–7). During the early stages of infection, *P. infestans* requires living host cells but later causes extensive necrosis of host tissue, a lifestyle that is known as hemibiotrophy. As with other biotrophic plant pathogens, processes associated with *P. infestans* pathogenesis are thought to include the suppression of host defense responses (3, 8, 9). In *P. infestans*, water-soluble glucans have been reported to suppress host defenses in a plant cultivar-specific manner (10–12). Nevertheless, the molecular basis of suppression of host defenses by *Phytophthora* remains poorly understood (3). It is tempting to speculate that unique classes of suppressor genes have been recruited to aid in infection and counteract host defenses during the evolution of pathogenesis in the oomycete lineage.

Parasitic eukaryotes often face inhospitable environments in their hosts. For example, parasites that colonize or transit through the mammalian digestive tract must adapt to the diverse and abundant array of proteases secreted in the gastric juices (13–15). Some of these parasites secrete inhibitors that target host proteases and may aid in survival and colonization of the host. For instance, the apicomplexan obligate parasite *Toxoplasma gondii* secretes TgPI-1 and TgPI-2, four-domain serine protease inhibitors of the Kazal family (15–19), and the intestinal hookworm *Ancylostoma ceylanicum* secretes an 8-kDa broad spectrum serine protease inhibitor of the Kunitz family (14). In plants, the apoplast (intercellular fluid) forms a protease-rich environment that is colonized by many pathogens, including *P. infestans* and the fungus *Cladosporium fulvum*. In tomato, apoplastic proteases are integral components of the plant defense response. Serine proteases of the P69 subtilase family have long been tied to pathogen defense, and two isoforms, P69B and P69C, are known as pathogenesis-related proteins (PR-7 class) (20–22). More recently, an apoplastic papain-like cysteine protease, Rcr3, was shown to be required for specific resistance to *C. fulvum* (23). In addition, several *C. fulvum* extracellular proteins are processed or degraded by host proteases in the apoplast, resulting in altered functionality (24, 25).

Despite the importance of extracellular proteases in plant defense, to date no protease inhibitor has been reported from microbial plant pathogens. In this paper, we describe and functionally characterize an extracellular protease inhibitor, EPI1, from *P. infestans*. EPI1 contains two domains with significant similarity to the Kazal family of serine protease inhibitors, which also occurs in many animal species and in apicomplexan parasites. *In vitro* studies indicated that recombinant EPI1 (rEPI1)[1] specifically inhibited subtilisin A among the major serine proteases. rEPI1 was further demonstrated to inhibit and interact with tomato P69B subtilisin-like serine protease.

* This work was supported by the Ohio Agricultural Research and Development Center Research Enhancement Grant Program and Syngenta Biotechnology Inc. Salaries and research support were provided by State and Federal Funds appropriated to the Ohio Agricultural Research and Development Center, the Ohio State University. The costs of publication of this article were defrayed in part by the payment of page charges. This article must therefore be hereby marked "*advertisement*" in accordance with 18 U.S.C. Section 1734 solely to indicate this fact.

‡ To whom correspondence should be addressed: Dept. of Plant Pathology, The Ohio State University-OARDC, 1680 Madison Ave., Wooster, OH 44691. Tel.: 330-263-3847; Fax: 330-263-3841; E-mail: kamoun.1@osu.edu.

[1] The abbreviations used are: rEPI1, recombinant EPI1; BTH, benzo-(1,2,3)-thiadiazole-7-carbothioic acid *S*-methyl ester; EST, expressed sequence tag; RT, reverse transcriptase.

The *epi1* and *P69B* genes were coordinately expressed and up-regulated during infection of tomato by *P. infestans*. Overall these results suggest that inhibition of tomato proteases by *P. infestans* EPI1 could form a novel type of defense-counter-defense mechanism between plants and microbial pathogens. In addition, this study points to a common virulence strategy between the oomycete plant pathogen *P. infestans* and mammalian parasites, such as the apicomplexan *T. gondii*.

MATERIALS AND METHODS

Phytophthora Strains and Culture Conditions—*P. infestans* isolate 90128 (A2 mating type, race 1.3.4.7.8.9.10.11) was used throughout the study. *P. infestans* 90128 was routinely grown on rye agar medium supplemented with 2% sucrose (26). For RNA extraction, plugs of mycelium were transferred to modified Plich medium (27) and grown for 2–3 weeks before harvesting.

Bacterial Strains and Plasmids—*Escherichia coli* XL1-Blue was used in this study and was routinely grown at 37 °C in LB medium (28). Plasmid pFLAG-EPI1 was constructed by cloning PCR-amplified DNA fragment corresponding to the mature sequence of EPI1 into the HindIII site of pFLAG-ATS (Sigma), a vector that allows secreted expression in *E. coli*. The oligonucleotides EPI1-F1 (5′-GCGAAGCTTCAAAGCCCGCAAGTCATCAG-3′) and EPI1-R1 (5′-GCGAAGCTTATCCCTCCTGCGGTGTC-3′) were used to amplify the fragment. The introduced HindIII restriction sites are underlined. The N-terminal sequence of the processed FLAG-rEPI1 protein is DYKDDDDKVKL**QSPQVISPAP**. . . . The FLAG epitope sequence is underlined, and the first 10 amino acids of mature EPI1 are shown in bold type.

Plant Growth, BTH Treatment, and Infection by P. infestans—Tomato (*Lycopersicon esculentum*) cultivar Ohio 7814 was used throughout the study and grown in pots at 25 °C, 60% humidity, under 16 h-light/8 h-dark cycle. We used the salicylic acid analog BTH to mimic pathogen infection. For BTH treatment, 10 ml of a 25 μg/ml BTH solution was applied to 3-week-old tomato plants by soil drench. Plants treated with 10 ml of water were used as controls. Leaves from BTH-treated and control plants were detached for isolation of intercellular fluids 6 days after treatment. Time courses of *P. infestans* infection of tomato leaves were performed exactly as described earlier (29). 10-μl droplets containing 1,000 zoospores of *P. infestans* were used to inoculate the underside of detached tomato leaves. Leaf discs of similar sizes were dissected from the inoculated regions while making sure that the inoculation spot is in the center of sampled area. Leaf discs were frozen in liquid nitrogen and stored at −80 °C for later use in RNA extraction. For isolation of intercellular fluids, tomato leaves were sprayed with zoospore suspensions at the concentration mentioned above (10^5/ml), and the intact leaves were collected at different time points for immediate preparation of intercellular fluids.

Isolation of Intercellular Fluids—Intercellular fluids were prepared using a 0.24 M sorbitol solution according to the method of de Wit and Spikman (30). The intercellular fluids were filter-sterilized (0.22 μM) and were used immediately or stored at −20 °C.

Sequence Analyses—GC counting was performed as described elsewhere (31). PexFinder and signal peptide predictions were performed as described by Torto *et al.* (32). Similarity searches were performed locally on an Intel Linux or a Mac OSX work station or through the internet on the NCGR (www.ncgr.org) and Whitehead Institute web servers (www-genome.wi.mit.edu/resources.html). Search programs included BLAST (33), and the similarity search programs implemented in the BLOCKS (34), pfam (35), SMART (36), and InterPro (37) websites. The examined sequence databases included GenBank™ nonredundant, dBEST, and TraceDB (38), PGC (39), SPC, a proprietary database of Syngenta Inc. containing ~75,000 ESTs from *P. infestans* (courtesy of the Syngenta *Phytophthora* Consortium, Research Triangle Park, NC), and the genome sequences of the fungal species *Aspergillus nidulans*, *Magnaporthe grisea*, *Neurospora crassa*, and *Fusarium graminearum* available through the Whitehead Institute Fungal Genome Initiative Databases (www-genome.wi.mit.edu/resources.html). Multiple alignments of the Kazal domains were conducted using the program CLUSTAL-X (40). The *P. infestans* and *Phytophthora brassicae* sequences described in this paper were deposited in GenBank™ under accession numbers AY586273-AY586284 and AY589086-AY589087, respectively. Other sequences were obtained from the NCBI nr, dBEST, or Trace Archive data bases (www.ncbi.nlm.nih.gov) (Table I).

RNA Isolation, Northern Blot, and RT-PCR Analyses—RNA isolation and Northern blot hybridizations were performed as described earlier (32). Probes for *epi1*, *actA*, and tomato α-tubulin were generated by random primer labeling using gel-purified fragments digested or PCR-amplified from the corresponding cDNA clones (Ref. 41 and this study). Probe for tomato *P69B* was generated from a gel-purified RT-PCR fragment amplified from total RNA isolated from infected tomato tissue. For RT-PCR, total RNA was treated with DNA-free™ (Ambion, Austin, TX) to remove contaminating DNA, and first-strand cDNAs were synthesized using the ThermoScript™ RT-PCR system from 5 μg of total RNA following the instructions of the manufacturer (Invitrogen). PCR amplifications were carried out with 0.005% of the cDNA product. The oligonucleotide primer pairs, P69A-RTF1 (5′-TGGCAGGTGGTGGAGTTCCGAGGG-3′) and P69A-RTR1 (5′-CATTGGATCAACAAAAGTGCAATTGG-3′), P69B-RTF1 (5′-CAGCACTCGGCCATGTAGCCAATGTT-3′) and P69B-RTR1 (5′-CTAGGCAGACACAACTGCAATTGGACTTC-3′), P69D-RTF1 (5′-TGCGAAGTATAAGTCTTCTCAGAGTTGC-3′), and P69D-RTR1 (5′-TCAGCAGACACTCTAACTGCAATTGGAC-3′), were designed to be gene-specific based on the published *P69* gene sequences (21) and were used for the amplification of *P69A*, *P69B*, and *P69D* sequences, respectively. The oligonucleotides EPI1-F1 and EPI1-R1, previously used for cloning *epi1* into pFLAG-ATS vector, were used to detect *epi1* transcripts by RT-PCR. Primer specificity was confirmed by sequencing the RT-PCR products. The expression of *P69A*, *P69B*, and *P69D* was controlled with primer pair EF1α-F1 (5′-GCTGCTGTAACAAGGTTTGCTTTAATTCG-3′) and EF1α-R1 (5′-CCAGCATCACACTGCACAGTTCACTTC-3′), which are specific for the constitutively expressed tomato elongation factor 1α gene (42). The expression of *epi1* was controlled with *P. infestans* elongation factor 2α gene using the primer pair described previously (43).

SDS-PAGE and Western Blot Analyses—Proteins were subjected to 10–15% SDS-PAGE as previously described (28). Following electrophoresis, the gels were stained with silver nitrate following the method of Merril *et al.* (44) or stained with Coomassie Brilliant Blue (28), or the proteins were transferred to supported nitrocellulose membranes (Bio-Rad) using a Mini Trans-Blot apparatus (Bio-Rad). Detection of antigen-antibody complexes was carried out with a Western blot alkaline phosphatase kit (Bio-Rad). Antisera to P69 subtilases were produced by immunizing rabbits with the keyhole limpet hemocyanin-conjugated peptide, H2N-TTHTPSFLGLQQNC-amide. The sequence underlined is located at the N terminus of mature P69B and P69D proteins (21) and was chosen for its highly antigenic characteristics and conservation among P69 proteins. Selection of peptides for highly antigenic characteristics, peptide synthesis, and conjugation, as well as antisera production, was performed by Rockland Immunochemicals (Gilbertsville, PA). In Western blot analyses, the antisera to the P69 peptide reacted only with ~70-kDa bands from tomato intercellular fluids.

Expression and Purification of rEPI1—Expression of rEPI from pFLAG-EPI1 was conducted as described previously (45). Overnight cultures of *E. coli* XL1-blue containing pFLAG-EPI1 were diluted (1:100) in LB medium containing ampicillin (50 μg/ml) and incubated at 37 °C. When the A_{600} of the cultures reached 0.6, isopropyl-β-D-thiogalactopyranoside was added to a final concentration of 0.4 mM. The cultures were further incubated for 5–6 h before processing. rEPI1 was recovered from the culture supernatant and was purified by immunoaffinity using gravity column packed with anti-FLAG M2 affinity gel (Sigma). The proteins were eluted with 0.1 M glycine, pH 3.5, and immediately equilibrated to neutral pH with 20 μl of 1 M Tris, pH 8.0, for each 1-ml eluted fraction. The protein concentrations were determined using the Bio-Rad protein assay. To determine the purity of rEPI1, 0.5 μg of the purified protein was run on a SDS-PAGE gel followed by staining with silver nitrate.

Assays of Protease Inhibition—Inhibition assays of commercial serine proteases by rEPI1 were performed by the colorimetric QuantiCleave™ Protease Assay Kit (Pierce). 20 pmol of rEPI1 was preincubated with 20 pmol of trypsin (Pierce), chymotrypsin (Sigma), or subtilisin A (Carlsberg) (Sigma), in a volume of 50 μl for 30 min at 25 °C, followed by incubation with 100 μl of succinylated casein (2 mg/ml) in 50 mM Tris buffer, pH 8, containing 20 mM $CaCl_2$ at room temperature for 20 min. Protease activity was measured as absorbance at 405 nm using a HTS 7000 Bio Assay Reader (PerkinElmer Life Sciences) 20 min after the addition of chromogenic reagent 2,4,6-trinitrobenzene sulfonic acid, which reacts with the primary amine of digested peptide and produces a color reaction that can be quantified by absorbance reader. Detailed kinetic analysis of Subtilisin A inhibition by rEPI1 was performed as follows. 2 pmol of subtilisin A was preincubated with increasing concentrations of rEPI1 in a volume of 50 μl for 15 min at 25 °C and was followed by the addition of 150 μl assay buffer: 50 mM Tris-Cl, pH 8.0, containing 2.5% Me_2SO, and 500 μM subtilisin chromogenic substrate Boc-Gly-Gly-Leu-pNA (Calbiochem, La Jolla, CA). The experiments were performed three times and in triplicate each

TABLE I
Predicted Kazal-like proteins from the oomycete plant pathogens P. infestans, P. sojae, P. ramorum, P. brassicae, and P. halstedii

Species	Protein	GenBank™ accession number	Signal peptide	Expression stage	Number of Kazal-like domains	P1 residue
P. infestans	EPI1	AY586273	Yes	Infected tomato	2	Asp, Asp
P. infestans	EPI2	AY586274	Yes	Mycelium, H_2O_2-treated	2	Asp, Asp
P. infestans	EPI3	AY586275	Yes	Genomic sequence	1	Glu
P. infestans	EPI4	AY586276	Yes	Mycelium, nitrogen starvation	3	Thr, Asp, Asp
P. infestans	EPI5	AY586277	Yes	Mating culture	1	Arg
P. infestans	EPI6	AY586278	NA[a]	Infected tomato	2	Asp, Asp
P. infestans	EPI7	AY586279	Yes	Genomic sequence	1	Asp
P. infestans	EPI8	AY586280	Yes	Genomic sequence	1	Asp
P. infestans	EPI9	AY586281	Yes	Mycelium, non-sporulating growth	1	Arg
P. infestans	EPI10	AY586282	Yes	Zoospores	3	Asp, Asp, Asp
P. infestans	EPI11	AY586283	Yes	Mating culture	1	Asp
P. infestans	EPI12	AY586284	Yes	Infected potato, germinating cysts	1	Ser
P. infestans	EPI13	317886987[b]	Yes	Genomic sequence	1	Glu
P. infestans	EPI14	317892389[b]	Yes	Genomic sequence	1	His
P. sojae	PsojEPI1	CF842223	Yes	Infected soybean	4	Ala, Glu, Lys, Ala
P. sojae	PsojEPI2	AAO24652	Yes	Mycelium	1	Glu
P. sojae	PsojEPI3	274204995[b]	Yes	Genomic sequence	3	Met, Asp, Glu
P. sojae	PsojEPI4	273523724[b]	Yes	Genomic sequence	3	Asp, Thr, Asp
P. sojae	PsojEPI5	273752552[b]	Yes	Genomic sequence	1	Arg
P. sojae	PsojEPI6	273759065[b]	Yes	Genomic sequence	1	Glu
P. sojae	PsojEPI7	324111439[b]	Yes	Genomic sequence	1	Asp
P. sojae	PsojEPI8	273566013[b]	Yes	Genomic sequence	1	Asp
P. sojae	PsojEPI9	274071280[b]	Yes	Genomic sequence	1	Arg
P. sojae	PsojEPI10	273704880[b]	Yes	Genomic sequence	1	Ala
P. sojae	PsojEPI11	324096913[b]	Yes	Genomic sequence	1	Asp
P. sojae	PsojEPI12	324106054[b]	Yes	Genomic sequence	1	Asp
P. ramorum	PramEPI1	303509335[b]	Yes	Genomic sequence	3	Asp, Met, Glu
P. ramorum	PramEPI4	324426165[b]	Yes	Genomic sequence	3	Asp, Thr, Asp
P. ramorum	PramEPI5	324427992[b]	Yes	Genomic sequence	1	Arg
P. ramorum	PramEPI9	303791515[b]	Yes	Genomic sequence	1	Arg
P. ramorum	PramEPI10	303447516[b]	Yes	Ggenomic sequence	3	Asp, Asp, Asp
P. ramorum	PramEPI11	303578321[b]	Yes	Ggenomic sequence	1	Asp
P. brassicae	PbraEPI1	AY589086	Yes	Mycelium, nitrogen starvation	2	Asn, Met
P. brassicae	PbraEPI2	AY589087	NA[a]	Mycelium	1	His
P. halstedii	PhaEPI1	CB174657	Yes	Infected sunflower	1	Arg

[a] NA, not available.
[b] Ti (Trace Identifier) number from NCBI Trace Archive (www.ncbi.nlm.nih.gov/Traces/trace.cgi).

time. Initial reaction velocities were measured by monitoring the absorbance change at 405 nm over reaction time using the HTS 7000 Bio Assay Reader (PerkinElmer Life Sciences). $K_{i\,app}$ was determined following the method described by Morris *et al.* (15). The slope of the linear plot of $[V_0/V_i] - 1$ *versus* [I] was estimated as $1/K_{i\,app}$. $K_{i\,app}$ was converted to K_i according to the formula $K_i = K_{i\,app}/(1 + [S]/K_m)$ (46). Varying concentrations of substrate were incubated with 2 pmol of subtilisin A in a total volume of 200 μl under the conditions described above, and the initial velocities were measured by monitoring the absorbance at 405 nm. The K_m was determined graphically by double-reciprocal Lineweaver-Burk plots of 1/[v] *versus* 1/[s].

Inhibition assays of plant proteases by rEPI1 were carried out with the QuantiCleave™ Protease Assay Kit (Pierce) and in-gel protease assays using the Bio-Rad zymogram buffer system. For the first method, 50 μl of intercellular fluids were preincubated with or without 10 pmol of rEPI1 at 25 °C for 30 min, and the protease activities were subsequently measured. For the in-gel protease assays, 10 pmol of rEPI1 were preincubated with 8 μl of intercellular fluids for 30 min at 25 °C and then mixed with zymogram sample buffer and loaded on a 10% SDS-polyacrylamide gel without boiling or addition of reducing reagents. Following electrophoresis, the gel was incubated in 1× zymogram renaturation buffer for 30 min. Then the gel was incubated in 1× zymogram development buffer for 4 h at 37 °C before staining with 0.5% Coomassie Brilliant Blue.

Coimmunoprecipitation—Coimmunoprecipitation of rEPI1 and tomato intercellular fluid proteins was performed using the FLAG-tagged protein immunoprecipitation kit (Sigma) following the manufacturer's instructions. 100 pmol of purified rEPI1 were preincubated with 200 μl of tomato intercellular fluid for 30 min at 25 °C. 50 μl of anti-FLAG M2 resin was added and incubated at 4 °C for 2 h with gentle shaking. The precipitated protein complexes were eluted in 60 μl of FLAG peptide solution (150 ng/μl) and were analyzed by SDS-PAGE and Western blot analyses.

Tandem Mass Spectrometric Sequencing—Tandem mass spectrometric sequencing was performed at the proteomics facility of The Cleveland Clinic Foundation (Cleveland, OH). The selected protein band was cored from the gel, and protein digestion was carried out as previously described (47). The liquid chromatography-mass spectrometry system used is a Finnigan LCQ-Deca ion trap mass spectrometer system with a Protana microelectrospray ion source interfaced to a self-packed 10 cm × 75 μm Phenomenex Jupiter C18 reversed-phase capillary chromatography column. 2-μl volumes of the peptide extract were injected, and the peptides were eluted from the column by an acetonitrile, 0.05 M acetic acid gradient at a flow rate of 0.2 μl/min. The microelectrospray ion source was operated at 2.5 kV. The digest was analyzed using the data-dependent multitask capability of the instrument resulting in ~1000 collision-induced dissociation spectra of ions ranging in abundance over several orders of magnitude. The data were analyzed by using all collision-induced dissociation spectra collected in the experiment to search the NCBI nonredundant data base with the search program TurboSequest. All matching spectra were verified by manual interpretation.

RESULTS

EPI1 Belongs to the Kazal Family of Protease Inhibitors—We mined an EST data set generated from tomato leaves 3 days after infection with *P. infestans* using two methods: 1) GC counting to distinguish between *Phytophthora* and tomato sequences (31) and 2) PexFinder to identify cDNAs encoding extracellular proteins (32). 488 of 2808 ESTs examined showed a GC content higher than 53%. Of these 42 were predicted to encode extracellular proteins using the criteria of Torto *et al.* (32). These ESTs were then annotated by similarity and motif searches against public databases. One EST, PC064G6 (GC content, 57.4%), showed similarity to proteins of the Kazal serine protease inhibitor family. DNA sequencing of the full cDNA revealed an open reading frame of 450 bp corresponding to a predicted translated product of 149 amino acids (Fig. 1*A*). SignalP (48) analysis of the predicted protein identified a 16-

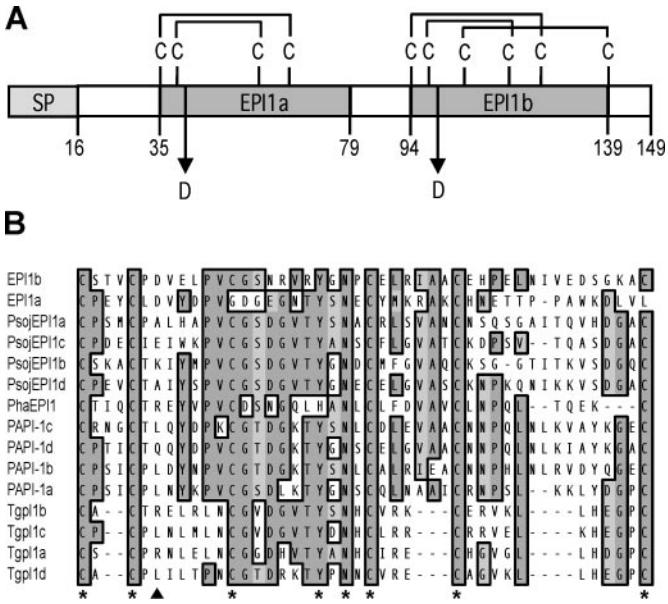

FIG. 1. **EPI1 belongs to the Kazal family of serine protease inhibitors.** *A*, schematic representation of EPI1 structure. The signal peptide (*SP*) and two Kazal domains (*EPI1a* and *EPI1b*) are shown in *gray*. The *numbers* indicate the positions of amino acid residues starting from the N terminus. The cysteine residues corresponding to the two Kazal domains are indicated by *C*, and the disulfide linkages predicted based on the structure of other Kazal domains are shown. The positions of the P1 aspartate residues are indicated by *arrows*. *B*, sequence alignment of EPI domains with representative Kazal family inhibitor domains. Protein names correspond to protease inhibitors of the oomycetes *P. infestans* (*EPI1a* and *EPI1b*; this study), *P. sojae* (PsojEPI1a–d; this study), and *P. halstedii* (PhaEPI1; GenBank™ accession number CB174657), the crayfish *Pacifastacus leniusculus* (PAPI-1a–d; CAA56043), as well as the apicomplexan *T. gondii* (TgPI-1a–d; AF121778). Amino acid residues that define the Kazal family protease inhibitor domain are marked with *asterisks*. The predicted P1 residues are shown by the *arrowhead*.

amino acid signal peptide with a significant mean *S* value of 0.88 and hidden Markov model score of 0.97. Similarity searches of the predicted protein against the nonredundant database of GenBank™ using the BLASTP program (33) revealed significant matches to Kazal protease inhibitors with the best hit corresponding to the signal crayfish protease inhibitor PAPI-1 (*E* value = 10^{-10}). Searches against the InterPro database (37) revealed two domains similar to InterPro IPR002350 for Kazal inhibitors (Fig. 1*A*). Based on these analyses, we propose that the examined *P. infestans* cDNA is likely to encode a two-headed Kazal serine protease inhibitor, and we designated the cDNA *epi1* (extracellular protease inhibitor 1).

Proteins with Kazal Domains Are Diverse and Ubiquitous in Oomycetes—We used EPI1 and other Kazal domain sequences to search for Kazal-like motifs in sequence databases from oomycetes and other microbial plant pathogens (see "Material and Methods"). We failed to identify sequences similar to the Kazal domain in all examined fungal and bacterial databases, except for a predicted protein from the ammonia-oxidizing bacterium *Nitrosomonas europaea* (GenBank™ accession NP_841298) (49). On the other hand, we unraveled a total of 35 different putative proteins with 56 predicted Kazal-like domains (range, 1–4/protein) in five plant pathogenic oomycete species, *P. infestans*, *Phytophthora sojae*, *Phytophthora ramorum*, *P. brassicae*, and the downy mildew *Plasmopara halstedii* (Table I). These oomycete Kazal motifs were identified in ESTs from a variety of developmental stages, including host tissue infected with *P. sojae* and *P. halstedii*. We identified a putative full open reading frame sequence for 27 of the identified genes and the putative start codon for 33 of the genes. All of these 33 genes were predicted to have signal peptides based on SignalP (48, 50).

We used Clustal X (40) to generate a multiple alignment of representative oomycete Kazal domains with domains from signal crayfish PAPI-1 (the best hit in BLASTP searches against GenBank™ nonredundant database) and *T. gondii* TgPI1 (Fig. 1*B*). Amino acid residues defining the Kazal family signature, including the cysteine backbone, tyrosine, and asparagine residues, were highly conserved. The oomycete domain structure was usually C-$X_{3,4}$-C-X_7-C-X_6-Y-X_3-C-X_6-C-$X_{9,12,13,14}$-C. The first EPI1 domain was atypical and lacked Cys^3 and Cys^6 but retained the other four cysteines (Fig. 1*A*). The predicted active site P1, which is central to the specificity of Kazal inhibitors (51, 52), was variable with 10 different amino acids represented (Ala, Asp, Glu, His, Lys, Met, Asn, Arg, Ser, and Thr). Remarkably, half (28 of 56) the P1 residues, including those of EPI1, were aspartate (Asp), an uncommon P1 amino acid in other natural Kazal inhibitors. These results suggest that genes encoding proteins with Kazal domains are diverse and ubiquitous in plant pathogenic oomycetes.

EPI1 Inhibits the Serine Protease Subtilisin A—To determine whether EPI1 functions as a serine protease inhibitor as predicted by bioinformatic analyses, we expressed in *E. coli* and affinity-purified rEPI1 as a fusion protein with the FLAG epitope tag at the N terminus. Silver staining of the purified rEPI1 fraction after SDS-PAGE revealed a single band indicating high purity. Chymotrypsin, trypsin, and subtilisin A, representing three major classes of serine proteases, were selected for inhibition assays with the purified rEPI1. Protease activity was measured with or without EPI1. In repeated assays, rEPI1 was found to inhibit about 90% of the measured activity of subtilisin A but did not cause apparent inhibition of the other two proteases (Fig. 2*A*). Time courses of chromogenic substrate hydrolysis by subtilisin A in the presence of increasing amounts of rEPI1 were performed and indicated that rEPI1 inhibition followed a typical dose-response pattern (Fig. 2*B*). The inhibitory constant (K_i) for subtilisin A inhibition by rEPI1 was determined at 2.77 ± 1.07 nM. These results suggest that *epi1* encodes a functional protease inhibitor that specifically targets the subtilisin class of serine proteases.

EPI1 Inhibits BTH-induced Apoplastic Proteases from Tomato—In tomato, some members of the subtilisin-like family P69, namely P69B and P69C, are known to be induced by pathogens and stress treatments and are classified as PR proteins (PR-7 class) (20–22). To test whether rEPI1 inhibits PR-like proteases in tomato, the salicylic acid analog BTH was applied to tomato plants to induce defense-related proteases. In-gel protease assays of tomato leaf intercellular fluid from both H_2O-treated and BTH-treated plants revealed that, as expected, BTH induced the production of abundant extracellular proteases in tomato that migrated as two separate but close bands (Fig. 3*A*). Inhibition assays revealed that rEPI1 dramatically inhibited these BTH-induced proteases as well as partially inhibited a constitutive protease. The total endoprotease activity of tomato intercellular fluids was also measured in the absence or presence of rEPI1. Significant inhibition of endoprotease activity was observed and corresponded to 28 and 27% of total activity in control and BTH-treated tomato, respectively (Fig. 4).

EPI1 Interacts with Pathogenesis-related Subtilases of the Tomato P69 Subfamily—To identify the plant proteases targeted by rEPI1, coimmunoprecipitation was performed on tomato intercellular fluid incubated with rEPI1 using FLAG antibody covalently linked agarose beads. In addition to rEPI1, two proteins were pulled down with the FLAG antibody only in the presence of rEPI1 (Fig. 5*A*). These two proteins exhibited a

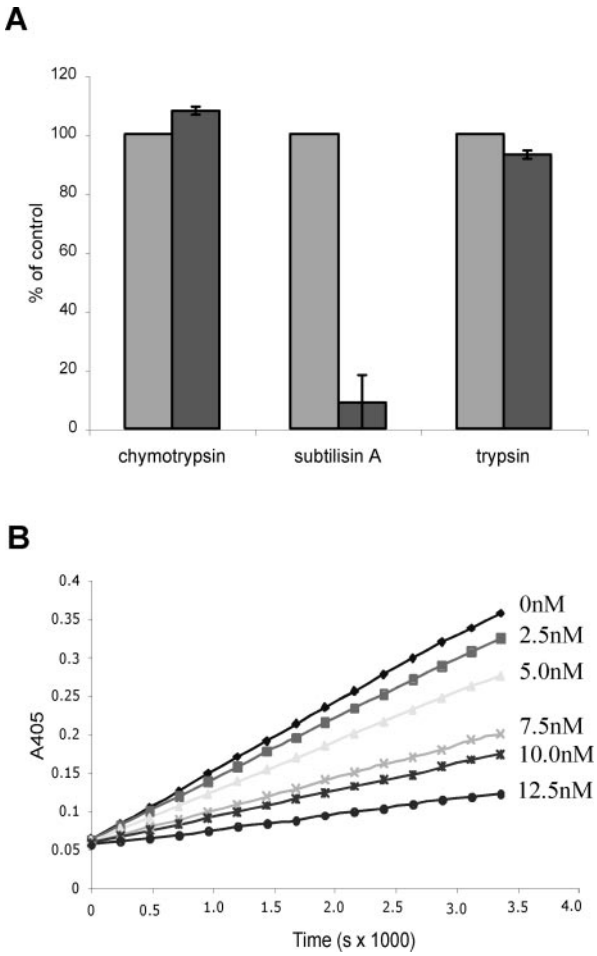

FIG. 2. **rEPI1 inhibits subtilisin A.** *A*, protease activity of chymotrypsin, subtilisin A, and trypsin in the absence (*gray columns*) or presence of rEPI1 (*black columns*). The activities were determined using the QuantiCleave™ protease assay kit as described under "Materials and Methods." Activity is expressed as a percentage of total protease activity in the absence of protease inhibitors. The *bars* correspond to the means of three independent replications of one representative experiment of three performed. The *error bars* represent the standard errors calculated from the three replications. *B*, time course of substrate hydrolysis by subtilisin A in the presence of varying concentrations of rEPI1. Protease activity was measured as absorbance at 405 nm based on hydrolysis of a chromogenic substrate. The final concentration of subtilisin A is 10 nM. The concentrations of rEPI1 are indicated next to the *curves*.

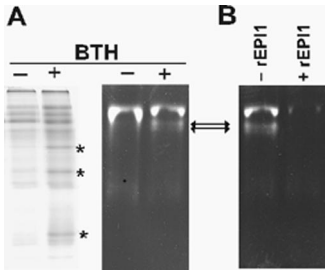

FIG. 3. **rEPI1 inhibits BTH-induced tomato proteases.** *A*, intercellular fluids obtained from water-treated (−) and BTH-treated (+) tomato plants were run on SDS-PAGE gel followed by staining with Coomassie Brilliant Blue (*left panel*) or were used in zymogen in-gel protease assays (*right panel*). The *asterisks* represent known pathogenesis-related proteins PR1, PR3, and PR2 (from *bottom* to *top*) and confirm the induction of defense responses by BTH. The *arrows* indicate BTH-induced protease activities that migrated as two close bands. *B*, inhibition of tomato proteases by rEPI1. Intercellular fluids from BTH-treated tomato leaves were incubated in the absence (− *rEPI1*) or presence of rEPI1 (+ *rEPI1*) and then analyzed using zymogen in-gel protease assays. The *arrows* indicate the BTH-induced protease bands.

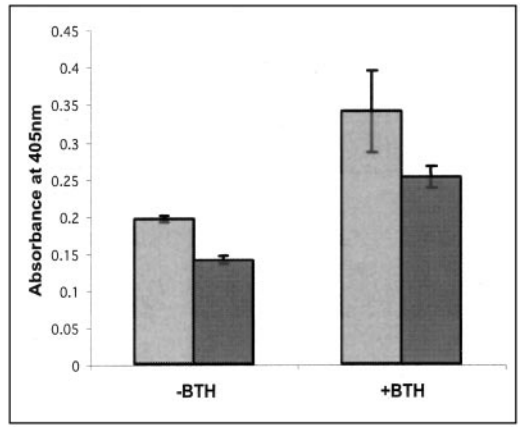

FIG. 4. **rEPI1 inhibition of total protease activity from tomato intercellular fluids.** Total protease activity of Intercellular fluids obtained from water-treated (−*BTH*) and BTH-treated (+*BTH*) tomato plants was measured in the absence (*gray columns*) or presence (*black columns*) of rEPI1 using the QuantiCleave™ protease assay kit as described under "Materials and Methods." Activity is expressed as absorbance at 405 nm. The *bars* correspond to the means of three independent replications of one representative experiment of three performed. The *error bars* represent the standard errors calculated from the three replications.

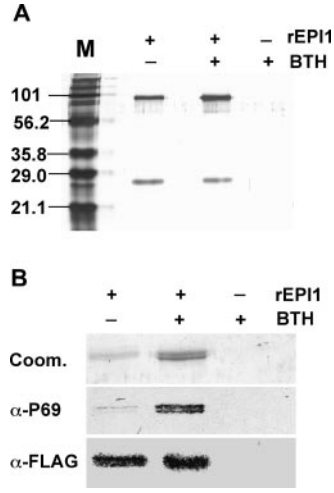

FIG. 5. **Coimmunoprecipitation of rEPIs and P69 subtilases using FLAG antisera.** *A*, eluates from coimmunoprecipitation of rEPI1 with proteins in tomato intercellular fluids were run on SDS-PAGE gel followed by staining with silver nitrate. The *numbers* on the *left* indicate the molecular masses of the marker proteins in kDa. *rEPI1* indicates whether or not rEPI1 was added to the reaction mix. *BTH* indicates whether or not the intercellular fluids were obtained from plants treated with BTH. The lower molecular mass band corresponds to rEPI1, and the high molecular mass bands correspond to the rEPI1-interacting protein(s). *B*, the same eluate samples were run on SDS-PAGE gel followed by staining with Coomassie Brilliant Blue (*Coom.*) or immunoblotting with antisera raised against a peptide specific for the tomato P69 family (α-*P69*), and FLAG (α-*FLAG*), respectively. The *top two panels* (*Coom.* and α-*P69*) correspond to the high molecular mass bands of *A*, whereas the *bottom panel* (α-*FLAG*) corresponds to the low molecular mass band.

similar molecular mass of ~70 kDa (Fig. 5*A*) and were more abundant in BTH-induced intercellular fluid (Fig. 5*B*). These results prompted us to test whether these proteins could be tomato P69 subtilisin-like proteases. Western blot analyses with antisera raised against a peptide specific to P69 subtilisin-like proteases strongly interacted with both bands, suggesting that rEPI1 interacts with P69 subtilases of tomato (Fig. 5*B*). To confirm the results obtained with the Western blot and further identify which P69 isoforms are the main targets of rEPI1, the two closely migrated protein bands (Fig. 5) were cored from the

*MGLLKILLVFIFCSFQWPTIQ*SNLETYIVHVESPESLVTTQSLLTDLGSY
YLSFLPKTATTISSSGNEEAATMIYSYHNVMTGFAARLTAEQVKEMEKKH
GFVSAQKQRILSLHTTHTPSFLGLQQNMGVWKDSNYGKGVIIGVIDTGII
PDHPSFSDVGMPPPPAKWKGVCESNFTNKCNNKLIGARSYQLGNGSPIDS
IGHGTHTASTAAGAFVK**GANVYGNADGTAVGVAPLAHIAIYK**VCNSVGCS
ESDVLAAMDSAIDDGVDILSMSLSGGPIPFHR**DNIAIGAYSATERG**ILVS
CSAGNSGPSFITAVNTAPWILTVGASTLDRKIKATVK**LGNGEEFEGESAY**
RPKISNATFFTLFDAAK**NAKDPSETPYCKRGSLTDPAIKGK**IVLCSALGH
VANVDKGQAVKDAGGVGMIIINPSQYGVTKSADAHVLPALVVSAADGTKI
LAYMNSTSSPVATIAFQGTIIGDK**NAPMVAAFSSRGPSR**ASPGILKPDII
GPGANILAAWPTSVDDNKNTKSTFNIISGTSMSCPHLSGVAALLK**CTHPD**
WSPAVIKSAMMTTADTLNLANSPILDEKLLPADIYAIGAGHVNPSRANDP
GLVYDTPFEDYVPYLCGLKYTDQQVGNLIQRRVNCSEVKSILEAQLNYPS
FSIFGLGSTPQTYTR**TVTNVGDATSSYK**VEVASPEGVAIEVEPSELNFSE
LNQK**LTYQVTFSK**TTNSSNPEVIEGFLKWTSNRHSVR**SPIAVVSA**

FIG. 6. **Tandem mass spectrometry identifies P69B as the main target of rEPI1.** The amino acid sequence of P69B subtilisin-like protease precursor is shown with the signal peptide sequence in *italics* and the propeptide domain sequence in *gray*. The 21 peptides sequenced by tandem mass spectrometry are shown in *bold type*. Each sequenced peptide ends with an Arg or a Lys residue, which is highlighted in *bold italics*. *Underlined sequences* are specific to P69B among the known P69 isoforms.

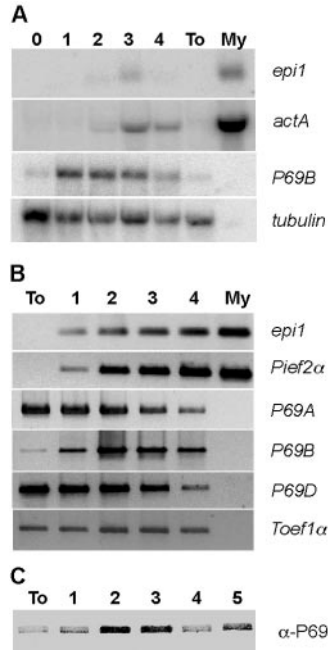

FIG. 7. **The *epi1* and *P69* genes are concurrently expressed during colonization of tomato by *P. infestans*.** *A*, time course of expression of *P. infestans epi1* and *actA* and tomato *P69B* and tubulin during colonization of tomato by *P. infestans*. Total RNA isolated from infected leaves of tomato, 0, 1, 2, 3, or 4 days after inoculation, from noninfected leaves (*To*), and from *P. infestans* mycelium grown in synthetic medium (*My*) was hybridized with probes from the four genes. The approximate sizes of the transcripts are ~600 nucleotides for *epi1*, 1600 nucleotides for *actA*, and 2500 nucleotides for *P69B* and *tubulin*. *B*, RT-PCR analysis of *epi1*, *P69A*, *P69B*, and *P69D* expression during colonization by *P. infestans*. Total RNA from a time course similar to the one described in *A* was used in RT-PCR amplifications as described in the text. Amplification of *P. infestans* elongation factor 2α (*Pief2α*) and tomato elongation factor 1α (*Toef1α*) were used as controls to determine the relative expression of *epi1* and *P69* genes, respectively. *C*, Western blot analyses of tomato P69 subtilases during colonization by *P. infestans*. The time course is as described for *A*. Equal volumes of intercellular fluids were obtained from infected tomato leaves, subjected to SDS-PAGE, and immunoblotted with P69 antisera (α-*P69*).

Coomassie Blue-stained SDS-PAGE gel as one sample and analyzed by tandem mass spectrometry. A total of 21 trypsin-digested peptides were sequenced and perfectly matched the subtilisin-like protease P69B (GenBank™ accession number T07184 or CAA76725) (Fig. 6). Of these 21 peptides, 13 peptides were specific to P69B and did not match any of the other five known P69 isoforms. At this stage it cannot be ruled out that the two closely migrated protein bands contain other isoforms in minor amounts, but the results from the tandem mass spectrometry clearly showed that P69B is the main target of rEPI1.

The epi1 and P69B Gene Are Concurrently Expressed during Infection of Tomato by P. infestans—Expression pattern of both *epi1* and *P69* genes during infection of tomato by *P. infestans* was studied by Northern blot and RT-PCR analyses. The *epi1* gene displayed the highest mRNA levels 3 days post-inoculation and was moderately up-regulated (approximately 2× based on PhosphorImager quantification) compared with *in vitro* grown mycelium and relative to the constitutive *actA* gene (Fig. 7*A*). Semi-quantitative RT-PCR analyses confirmed these results (Fig. 7*B*). The expression of *P69* protease genes was induced after inoculation with *P. infestans* and attained the highest level 2 and 3 days after inoculation (Fig. 7*A*). Semi-quantitative RT-PCR amplifications using primers specific for *P69A*, *P69B*, and *P69D*, indicated that the pathogenesis-related *P69B* gene is the only gene that is up-regulated during interaction with *P. infestans* (Fig. 7*B*). We could not assess the expression of *P69C*, the other pathogenesis-related gene of the *P69* family (21), because we repeatedly failed to amplify *P69C* from tomato cultivar Ohio 7814 based on published sequences. Increase in P69 protein during infection of tomato by *P. infestans* was also noted by Western blot analyses with P69 antisera of intercellular fluids obtained from a time course infection (Fig. 7*C*). Altogether, these results suggest that *epi1* and *P69* genes are concurrently expressed during infection and support the possibility of direct interaction between *P. infestans* EPI1 and plant P69 proteases, particularly P69B, at the infection interface.

DISCUSSION

Plant pathogens manipulate biochemical and physiological processes in their host plants through a diverse array of virulence or avirulence molecules, known as effectors. In susceptible plants, biotrophic plant pathogens produce effectors that promote infection by suppressing defense responses. Here, we describe EPI1, a two-domain extracellular protease inhibitor from *P. infestans* that inhibits apoplastic subtilases of tomato, namely the PR proteins P69. Based on its biological activity and expression pattern, EPI1 may function as a disease effector molecule and may play an important role in *P. infestans* colonization of host apoplast.

Suppression of host defenses is thought to play a critical role in plant-microbe interactions, especially those involving biotrophic pathogens that require live plant cells to establish a successful infection (8, 53). Nonetheless, only a few pathogen molecules that suppress host defenses have been identified. Examples include tomatinase, a saponin-detoxifying enzyme from the fungal pathogen *Septoria lycopersici* that was recently shown to indirectly suppress host defense responses through its degradation products (9). *P. sojae* secretes glucanase inhibitor proteins that inhibit a soybean endo-β-1,3-glucanase and are thought to function as counterdefensive molecules that inhibit the degradation of β-1,3/1,6-glucans in the pathogen cell wall and/or the release of defense-eliciting oligosaccharides by host endo-β-1,3 glucanases (54). *P. infestans* and other *Phytophthora* species produce water-soluble glucans that suppress induction of host defense responses (10–12). Here, we describe a novel class of pathogen suppressors of plant defense response,

namely extracellular protease inhibitors that directly interact with and inhibit host proteases. This interaction could form another type of defense-counterdefense mechanism between plants and microbial pathogens

We scanned GenBank™ and several other sequence data bases for the occurrence of Kazal-like domains. The examined data sets included the full genome sequence of several plant pathogenic bacteria and fungi. A 235-amino acid protein from the ammonia-oxidizing bacterium *N. europaea* (GenBank™ accession NP_841298) was the only bacterial or fungal protein with significant similarity to the Kazal motif. In sharp contrast, 56 Kazal-like motifs were detected in 35 predicted proteins of five plant pathogenic oomycete species, *P. infestans*, *P. sojae*, *P. ramorum*, *P. brassicae*, and *P. halstedii* (Table I). Interestingly, oomycete Kazal motif genes are often expressed during host colonization. Five of the identified sequences were from cDNAs obtained from infected plant tissue corresponding to diverse oomycete pathosystems: *P. infestans* tomato/potato, *P. sojae* soybean, and *P. halstedii* sunflower. Taken together, the common occurrence of Kazal motifs in several plant pathogenic oomycetes, their *in planta* expression, and the functional analyses of EPI1 suggest that inhibition of host proteases could be a conserved virulence strategy among oomycete pathogens. It remains unclear whether other plant pathogenic microbes have evolved inhibitors to counteract plant proteases. If so these inhibitors apparently belong to structural classes other than the Kazal inhibitor domain.

Several plant proteases have been linked to plant defense responses. In tomato, P69 and Rcr3 are two extracellular proteases that have been implicated in the defense response (20, 21, 23). The precise mode of action of these proteases remains unclear. They could degrade secreted proteins from the pathogen, thereby directly contributing to defense. Alternatively, plant proteases could contribute to defense signaling by processing endogenous or pathogen proteins to generate bioactive peptides. Future experiments will focus on determining whether EPI1 contributes to virulence by protecting other secreted proteins of *P. infestans* from proteolytic degradation in the host apoplast or by perturbing defense signaling in host plants.

P1 is the primary specificity-determining residue of Kazal inhibitors (51, 52). Remarkably, half (28 of 56) the predicted P1 residues of oomycete Kazal-like inhibitors, including two-thirds (14 of 21) of the *P. infestans* inhibitor domains, are aspartate. This is an uncommon P1 amino acid in natural Kazal inhibitors of animals and apicomplexans. This striking feature is remarkable in light of a recent finding that two oat proteases with caspase activity and specificity are subtilisin-like serine proteases that are involved in pathogen-induced programmed cell death (55). Coffeen and Wolpert (55) coined these enzymes saspases because their active-site residue is a serine and they require an asparate residue in the P1 position of the substrate. Saspases could be the enigmatic functional analogs of animal caspases that have been tied to multiple cases of pathogen-induced programmed cell death (56). *Phytophthora* EPIs that carry aspartate as the P1 residue might therefore target plant saspases and suppress host cell death. This engaging hypothesis will warrant a close examination.

Proteins with Kazal inhibitor domains have a restricted taxonomic distribution as determined by our exhaustive search of sequence and protein motif data bases. In addition to oomycetes, they are mainly found in animal species and in apicomplexans such as *T. gondii*, a parasite that transits through the mammalian digestive tract (15–19). An interesting analogy can be made between plant apoplasts and mammalian digestive tracts. Both environments are rich in proteases but nevertheless are colonized by a variety of microbial pathogens. Apparently, *P. infestans* and *T. gondii*, even though phylogenetically unrelated, have independently recruited secreted proteins of the Kazal family to inhibit host proteases and adapt to protease-rich host environments. Interestingly, unlike the *T. gondii* inhibitors (15, 19), EPI1 does not inhibit trypsin and chymortrypsin, suggesting that coevolution between the inhibitors and their target proteases may have shaped the inhibitor specificity. Future structural and functional characterization of Kazal protease inhibitors from animal and plant pathogens will shed some light on interesting questions on the evolution of pathogenesis in eukaryotic microbes and the coevolution of pathogen effectors with host targets.

Acknowledgments—We are grateful to Caitlin Cardina, Shujing Dong, Diane Kinney, and Kristin Wille for technical assistance; Margaret Redinbaugh and Saskia Hogenhout for valuable advice on the protein work; Tea Meulia and the staff of the Ohio Agricultural Research and Development Center Molecular and Cellular Imaging Center for help with DNA sequencing; and Andrew Keightley and Mike Kinter for performing the tandem mass spectrometry experiment. We thank the Syngenta *Phytophthora* Consortium for access to sequences of *P. infestans* and *P. brassicae*.

REFERENCES

1. Sogin, M. L., and Silberman, J. D. (1998) *Int. J. Parasitol.* **28,** 11–20
2. Margulis, L., and Schwartz, K. V. (2000) *Five Kingdoms: An Illustrated Guide to the Phyla of Life on Earth*, pp. 168–171, W. H. Freeman and Co., New York
3. Kamoun, S. (2003) *Eukaryotic Cell* **2,** 191–199
4. Birch, P. R. J., and Whisson, S. (2001) *Mol. Plant Pathol.* **2,** 257–263
5. Smart, C. D., and Fry, W. E. (2001) *Biol. Invas.* **3,** 235–243
6. Ristaino, J. B. (2002) *Microbes Infect.* **4,** 1369–1377
7. Shattock, R. C. (2002) *Pest Manag. Sci.* **58,** 944–950
8. Heath, M. C. (2000) *Plant Mol. Biol.* **44,** 321–334
9. Bouarab, K., Melton, R., Peart, J., Baulcombe, D., and Osbourn, A. (2002) *Nature* **418,** 889–892
10. Sanchez, L. M., Ohno, Y., Miura, Y., Kawakita, K., and Doke, N. (1992) *Ann. Phytopathol. Soc. Japan* **58,** 664–670
11. Yoshioka, H., Hayakawa, Y., and Doke, N. (1995) *Ann. Phytopathol. Soc. Japan* **61,** 7–12
12. Andreu, A., Tonón, C., Van Damme, M., Van Damme, M., Huarte, M., Huarte, M., and Daleo, G. (1998) *Eur. J. Plant Pathol.* **104,** 777–783
13. Dubey, J. P. (1998) *Parasitology* **116,** 43–50
14. Milstone, A. M., Harrison, L. M., Bungiro, R. D., Kuzmic, P., and Cappello, M. (2000) *J. Biol. Chem.* **275,** 29391–29399
15. Morris, M. T., Coppin, A., Tomavo, S., and Carruthers, V. B. (2002) *J. Biol. Chem.* **277,** 45259–45266
16. Pszenny, V., Angel, S. O., Duschak, V. G., Paulino, M., Ledesma, B., Yabo, M. I., Guarnera, E., Ruiz, A. M., and Bontempi, E. J. (2000) *Mol. Biochem. Parasitol.* **107,** 241–249
17. Lindh, J. G., Botero-Kleiven, S., Arboleda, J. I., and Wahlgren, M. (2001) *Mol. Biochem. Parasitol.* **116,** 137–145
18. Pszenny, V., Ledesma, B. E., Matrajt, M., Duschak, V. G., Bontempi, E. J., Dubremetz, J. F., and Angel, S. O. (2002) *Mol. Biochem. Parasitol.* **121,** 283–286
19. Morris, M. T., and Carruthers, V. B. (2003) *Mol. Biochem. Parasitol.* **128,** 119–122
20. Tornero, P., Conejero, V., and Vera, P. (1997) *J. Biol. Chem.* **272,** 14412–14419
21. Jorda, L., Coego, A., Conejero, V., and Vera, P. (1999) *J. Biol. Chem.* **274,** 2360–2365
22. van Loon, L. C., and van Strien, E. A. (1999) *Physiol. Mol. Plant Pathol.* **55,** 85–97
23. Kruger, J., Thomas, C. M., Golstein, C., Dixon, M. S., Smoker, M., Tang, S., Mulder, L., and Jones, J. D. (2002) *Science* **296,** 744–747
24. Van den Ackerveken, G. F., Vossen, P., and De Wit, P. J. (1993) *Plant Physiol.* **103,** 91–96
25. Joosten, M. H. A. J., Vogelsang, R., Cozijnsen, T. J., Verberne, M. C., and de Wit, P. J. G. M. (1997) *Plant Cell* **9,** 367–379
26. Caten, C. E., and Jinks, J. L. (1968) *Can. J. Bot.* **46,** 329–347
27. Kamoun, S., Young, M., Glascock, C., and Tyler, B. M. (1993) *Mol. Plant Microbe Interact.* **6,** 15–25
28. Sambrook, J., Fritsch, E. F., and Maniatis, T. (1989) *Molecular Cloning: A Laboratory Manual*, 2nd Ed., Cold Spring Harbor Laboratory, Cold Spring Harbor, NY
29. Kamoun, S., van West, P., Vleeshouwers, V. G., de Groot, K. E., and Govers, F. (1998) *Plant Cell* **10,** 1413–1426
30. de Wit, P. J. G. M., and Spikman, G. (1982) *Physiol. Plant Pathol.* **21,** 1–11
31. Huitema, E., Torto, T. A., Styer, A., and Kamoun, S. (2003) in *Functional Genomics: Methods and Protocols* (Grotewold, E., ed) pp. 79–83, Humana Press, Totowa, NJ
32. Torto, T., Li, S., Styer, A., Huitema, E., Testa, A., Gow, N. A. R., van West, P., and Kamoun, S. (2003) *Genome Res.* **13,** 1675–1685
33. Altschul, S. F., Madden, T. L., Schaffer, A. A., Zhang, J., Zhang, Z., Miller, W., and Lipman, D. J. (1997) *Nucleic Acids Res.* **17,** 3389–3402
34. Henikoff, J. G., Greene, E. A., Pietrokovski, S., and Henikoff, S. (2000) *Nucleic*

Acids Res. **28,** 228–230
35. Bateman, A., Birney, E., Cerruti, L., Durbin, R., Etwiller, L., Eddy, S. R., Griffiths-Jones, S., Howe, K. L., Marshall, M., and Sonnhammer, E. L. (2002) *Nucleic Acids Res.* **30,** 276–280
36. Letunic, I., Goodstadt, L., Dickens, N. J., Doerks, T., Schultz, J., Mott, R., Ciccarelli, F., Copley, R. R., Ponting, C. P., and Bork, P. (2002) *Nucleic Acids Res.* **30,** 242–244
37. Apweiler, R., Attwood, T. K., Bairoch, A., Bateman, A., Birney, E., Biswas, M., Bucher, P., Cerutti, L., Corpet, F., Croning, M. D., Durbin, R., Falquet, L., Fleischmann, W., Gouzy, J., Hermjakob, H., Hulo, N., Jonassen, I., Kahn, D., Kanapin, A., Karavidopoulou, Y., Lopez, R., Marx, B., Mulder, N. J., Oinn, T. M., Pagni, M., and Servant, F. (2001) *Nucleic Acids Res.* **29,** 37–40
38. Karsch-Mizrachi, I., and Ouellette, B. F. (2001) *Methods Biochem. Anal.* **43,** 45–63
39. Waugh, M., Hraber, P., Weller, J., Wu, Y., Chen, G., Inman, J., Kiphart, D., and Sobral, B. (2000) *Nucleic Acids Res.* **28,** 87–90
40. Thompson, J. D., Gibson, T. J., Plewniak, F., Jeanmougin, F., and Higgins, D. G. (1997) *Nucleic Acids Res.* **25,** 4876–4882
41. Unkles, S. E., Moon, R. P., Hawkins, A. R., Duncan, J. M., and Kinghorn, J. R. (1991) *Gene* (*Amst.*) **100,** 105–112
42. Shewmaker, C. K., Ridge, N. P., Pokalsky, A. R., Rose, R. E., and Hiatt, W. R. (1990) *Nucleic Acids Res.* **18,** 4276
43. Torto, T. A., Rauser, L., and Kamoun, S. (2002) *Curr. Genet.* **40,** 385–390
44. Merril, C. R., Goldman, D., Sedman, S. A., and Ebert, M. H. (1981) *Science* **211,** 1437–1438
45. Kamoun, S., van West, P., de Jong, A. J., de Groot, K., Vleeshouwers, V., and Govers, F. (1997) *Mol. Plant-Microbe Interact.* **10,** 13–20
46. Delaria, K. A., Muller, D. K., Marlor, C. W., Brown, J. E., Das, R. C., Roczniak, S. O., and Tamburini, P. P. (1997) *J. Biol. Chem.* **272,** 12209–12214
47. Hanna, S. L., Sherman, N. E., Kinter, M. T., and Goldberg, J. B. (2000) *Microbiology* **146,** 2495–2508
48. Nielsen, H., Engelbrecht, J., Brunak, S., and von Heijne, G. (1997) *Int. J. Neural Syst.* **8,** 581–599
49. Chain, P., Lamerdin, J., Larimer, F., Regala, W., Lao, V., Land, M., Hauser, L., Hooper, A., Klotz, M., Norton, J., Sayavedra-Soto, L., Arciero, D., Hommes, N., Whittaker, M., and Arp, D. (2003) *J. Bacteriol.* **185,** 2759–2773
50. Nielsen, H., and Krogh, A. (1998) *Proceedings of the Sixth International Conference on Intelligent Systems for Molecular Biology*, pp. 122–130, American Association for Artificial Intelligence Press, Menlo Park, CA
51. Lu, W., Apostol, I., Qasim, M. A., Warne, N., Wynn, R., Zhang, W. L., Anderson, S., Chiang, Y. W., Ogin, E., Rothberg, I., Ryan, K., and Laskowski, M., Jr. (1997) *J. Mol. Biol.* **266,** 441–461
52. Lu, S. M., Lu, W., Qasim, M. A., Anderson, S., Apostol, I., Ardelt, W., Bigler, T., Chiang, Y. W., Cook, J., James, M. N., Kato, I., Kelly, C., Kohr, W., Komiyama, T., Lin, T. Y., Ogawa, M., Otlewski, J., Park, S. J., Qasim, S., Ranjbar, M., Tashiro, M., Warne, N., Whatley, H., Wieczorek, A., Wieczorek, M., Wilusz, T., Wynn, R., Zhang, W., and Laskowski, M., Jr. (2001) *Proc. Natl. Acad. Sci. U. S. A.* **98,** 1410–1415
53. Heath, M. C. (1995) *Can. J. Bot.* **73,** (Suppl. 1) S616–S623
54. Rose, J. K., Ham, K. S., Darvill, A. G., and Albersheim, P. (2002) *Plant Cell* **14,** 1329–1345
55. Coffeen, W. C., and Wolpert, T. J. (2004) *Plant Cell* **16,** 857–873
56. Woltering, E. J., van der Bent, A., and Hoeberichts, F. A. (2002) *Plant Physiol.* **130,** 1764–1769